NASA–Ames University Consortium

Prismatic Grid Generation and Validation
NCC2–5004

Summary of Research

1 Improvement of Prismatic Grid Generation Algorithm

In this fully discrete approach to prismatic grid generation, improvement has been achieved in the formulation of the marching direction. The marching direction is obtained from the minimization of the sum of the squares of a subset of prisms having the marching edge in common. The functional reads:

$$I_i = \sum_{k \in K} (\vec{r}_i \cdot \vec{A}_k)^2 \tag{1}$$

where i is the node to update.

$\vec{r}_i$ is the marching vector.

K is the subset of base triangles whose intersection with the new shell tangent plane forms the largest convex polygon.

$\vec{A}_k$ is the surface vector for triangle k.

The marching direction obtained in this manner is always within the "admissibility cone" (all the volumes of the prisms attached to the marching vector are positive). However, it has been found numerically, by marching a large number of shells that the triangle "quality" was degrading with marching distance. Triangle "quality" is defined here as the smallest ratio of two adjacent edges in the triangularization.

A modification of the functional has been introduced which maintains the marching direction within the admissibility cone, but improves, as indicated by numerical experimentation, the mesh quality, and yields a stable asymptotic state.

The new functional reads:

$$\tilde{I}_i = \sum_{k \in K} \frac{1}{|A_k|^\alpha} (\vec{r}_i \cdot \vec{A}_k)^2 \tag{2}$$

The weighted factor $\frac{1}{|A_k|^\alpha}$ has been tested. The best value of α has been found to be $\alpha = 1$. The test case consists in the marching spherical shells

from an initially distorted triangular mesh on the sphere of radius $R = 1$. Such an initial distortion is shown on figure 1. The modification affects all the triangles attached to the pole which have been made smaller. Points like "a" have been moved to "a'", "b" to "b'" , etc... The sphere is "transparent" and the mesh on the opposite undistorted side is also visible "through" the sphere.

Figure 2 shows the evolution of triangle "quality" with shell distance. The shells have been marched to a radius $R = 1000$ with different step sizes $\Delta r = 0.1$ and 0.025. As can be seen, the quality improves and converges to a value between 0.4 and 0.5. On the same figure, other weighting factors are presented that clearly indicate breakdown of regularity with distance.

In conclusion, an improved scheme for the prismatic grid marching algorithm has been introduced which exhibits good asymptotic behavior without increasing the algorithm complexity. This new formulation improves the robustness of the method.

2 Prism/Tetrahedral Hybrid Approach

A viscous flow solution procedure for complex bodies using the prismatic grid in combination with tetrahedral grid is considered.

Step 1: A prismatic grid is generated to discretize the viscous region of the flow field. A grid generation algorithm is developed to accomplish this task.

Step 2: A tetrahedral grid is generated from the outer layer of the prismatic grid to the far field(See figure 3). The tetrahedra are meant for discretizing the inviscid flow field. An off-the-shelf tetrahedral grid generator(FELISA) is modified to do this job.

Step 3: We can now solve the Navier–Stokes equations on the prismatic grid and the Euler equations on the tetrahedral grid. A Navier–Stokes solver will be written for prismatic grids. It will treat the direction normal to the surface(the structured grid direction) implicitly while treating the other two directions explicitly. It will be shown that this semi–implicit method takes less number of iterations and less CPU time than an equivalent explicit method. The Euler solver will be a simple finite volume solver for a tetrahedral grid.

An integrated solution will be obtained by passing fluxes conservatively across the perfectly matching triangulated border between the two grids.

2.0.1 Tetrahedra

A NASA tetrahedral grid generator based on the advancing front idea called FELISA was used to generate tetrahedra shown in figure 3. An outer surface of a prismatic grid around an ellipsoid was provided with a far-field boundary(another ellipsoid of larger radii). FELISA successfully generated the required tetrahedra.

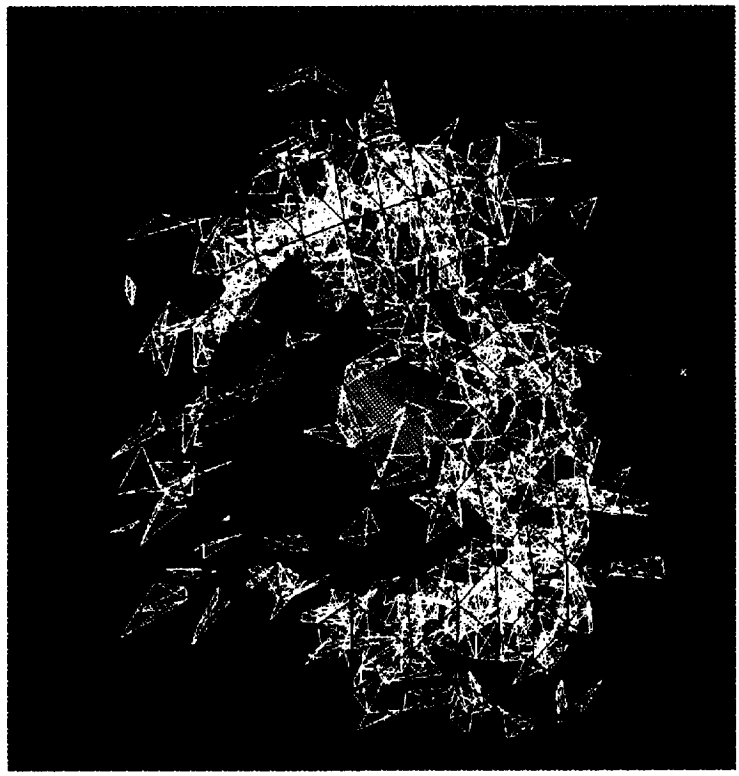

Figure 3: Selected tetrahedra between the outer most layer of a prismatic grid(solid) and a predefined outer boundary(green)

2.0.2 Prism/Tetrahedral Boundary

The boundary between the prismatic grid and the tetrahedral grid must match exactly for the flow solution procedure to be conservative. Two modifications to FELISA will be required in order to make sure that the outer

layer of the prismatic grid matches the initial front of the tetrahedral grid exactly.

One major modification is required to make sure that FELISA does not modify the initial front(the outer most surface of the prismatic grid) in its edge swapping cycle. Edge swapping is done in most advancing front codes to improve the quality of the tetrahedra where necessary.

The second modification has to do with identifying the boundary and the common points and faces on the boundary for later use in passing the flux from one grid to the other. This is mainly a book keeping problem.

2.1 Solution Validation

Two codes were written for method validation. The first code was a 2D finite difference Navier–Stokes code; written as a test platform to test the basic ideas such as the treatment of the normal direction implicitly. The other code was an inviscid solver for three dimensions. The results from both are presented below.

The following results were obtained from the 2D Navier–Stokes Solver.

Couette Flow:

A solution for the fully developed couette flow was obtained from the Navier–Stokes solver with the bottom plate fixed and the top plate moving at Mach 0.4 at a Re number of 100. The low Reynolds number allowed the solution of the equations without the addition of a lot of artificial viscosity, thus testing the validity of the viscous terms. Figure 4 shows the velocity vectors in one part of the couette. Note the linear profile which almost exactly matches the analytic solution.

Flat Plate:

The flat plate case was computed with the same code with a minimal amount of fourth order viscosity at $M = 0.4$ and $Re = 500$. The velocity magnitude contours are presented in figure 5. Some oscillations still remain in the solution and the fourth order viscosity needs more work to get higher Re solutions.

Three Dimensional Sphere:

The inviscid potential solver was used to compute flow around a sphere. The solution is presented in figure 6.

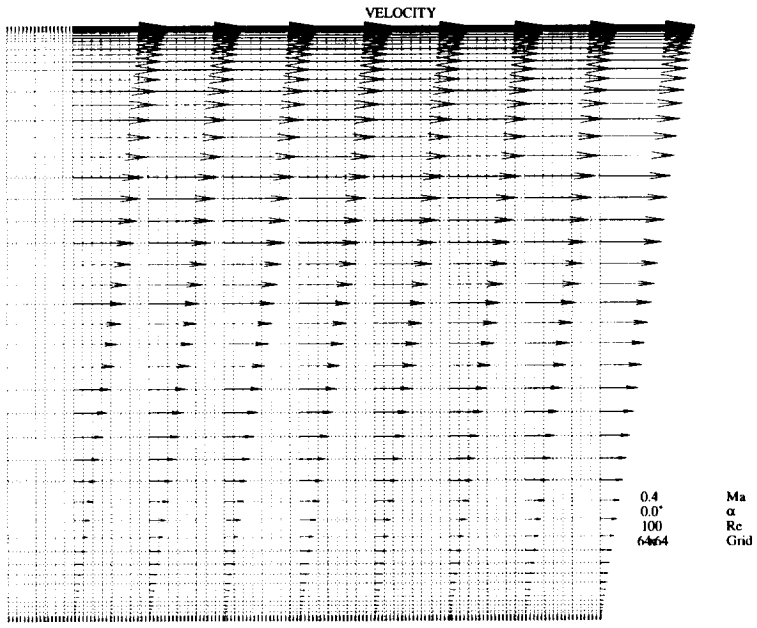

Figure 4: Numerical solution of a fully developed flow in a couette

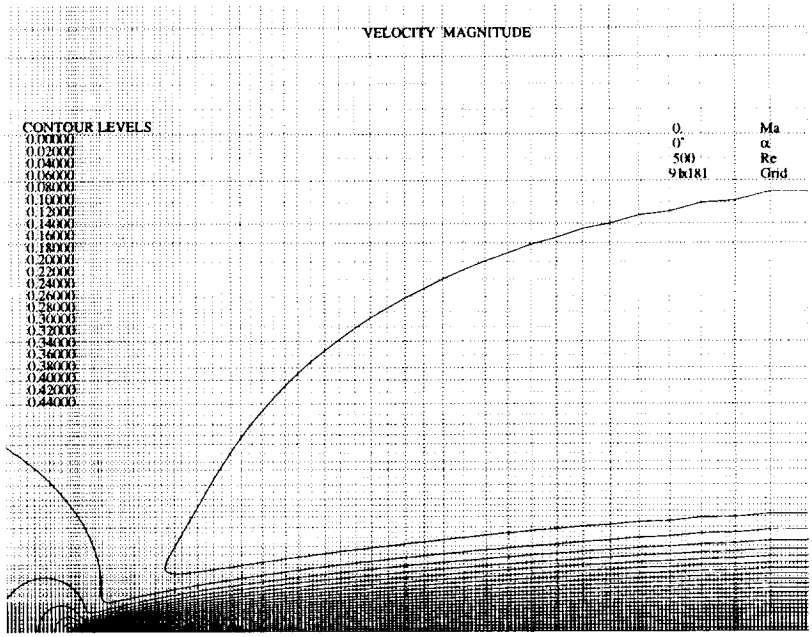

Figure 5: Numerical solution of viscous flow over a flat plate

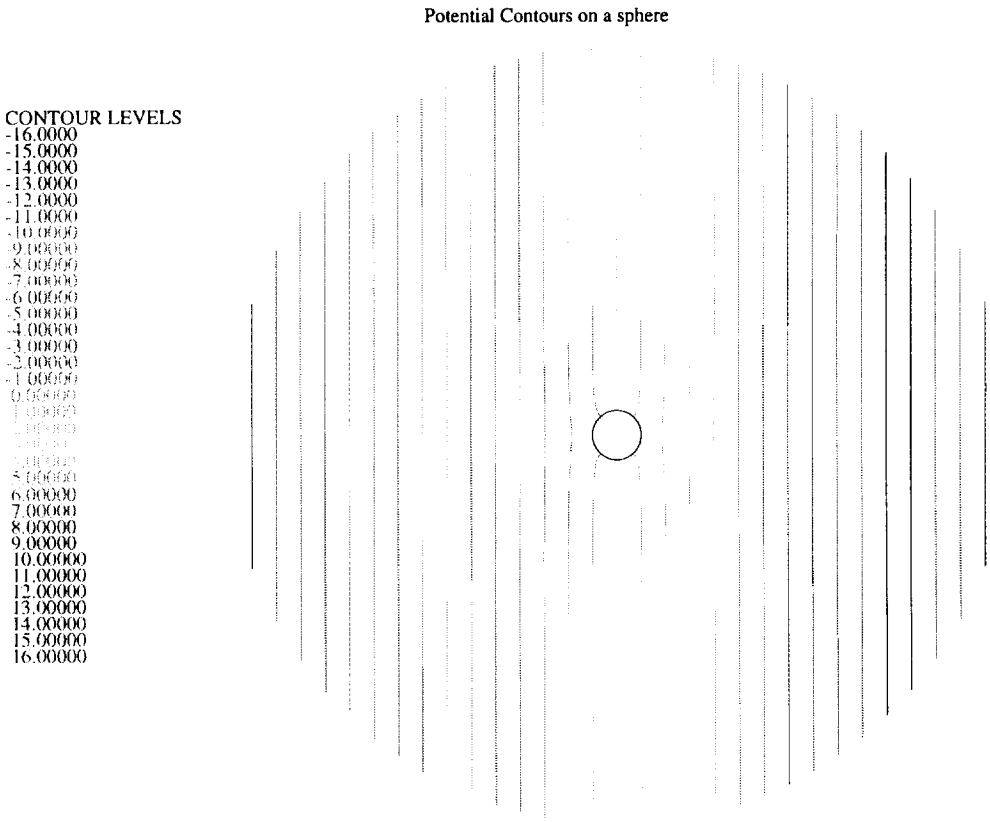

Figure 6: 2D cut from a numerical solution of potential flow over a sphere

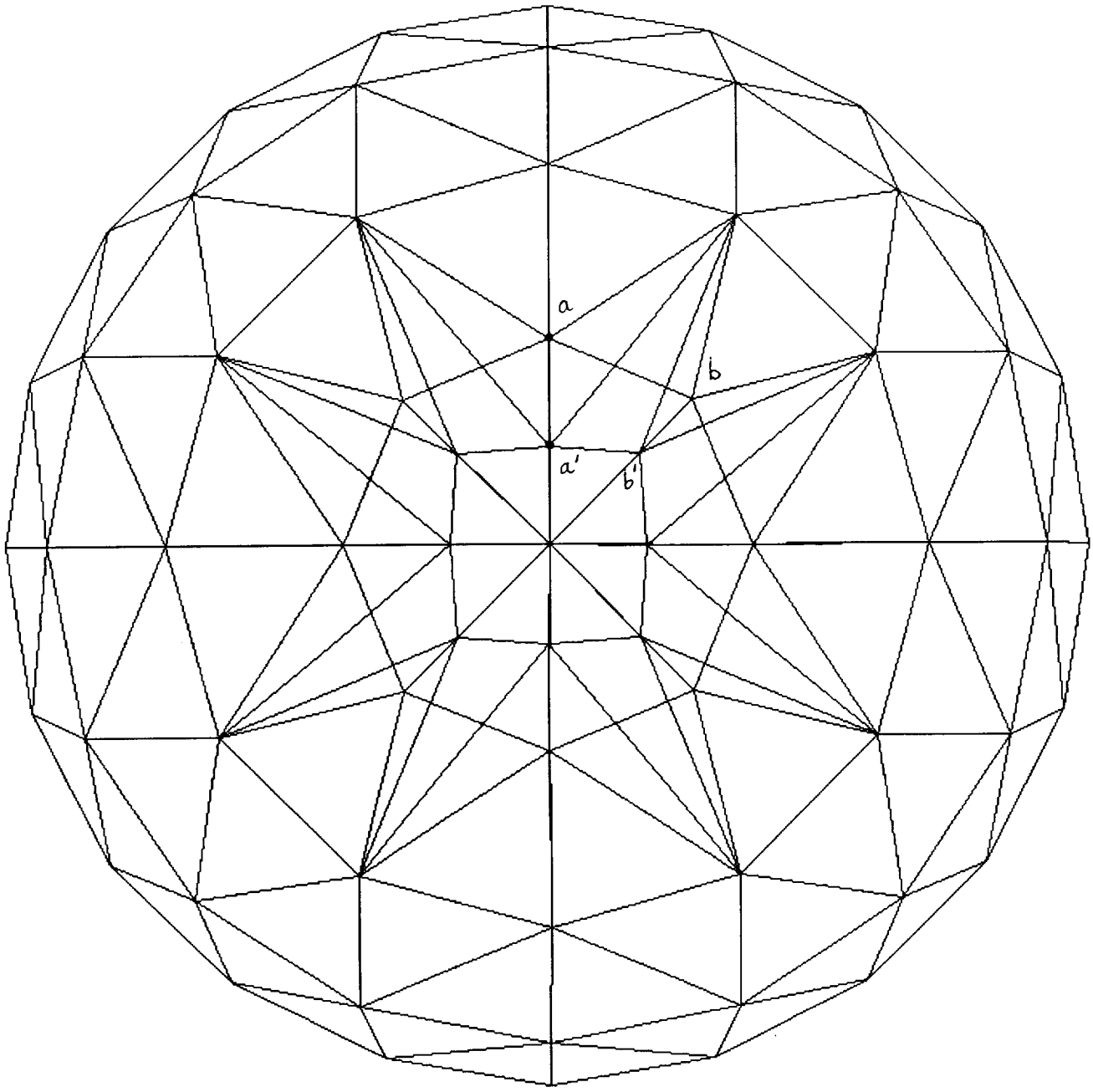

Figure 1. Initially distorted shell on unit sphere as seen from north pole. Undistorted mesh on southern hemisphere is "seen through"

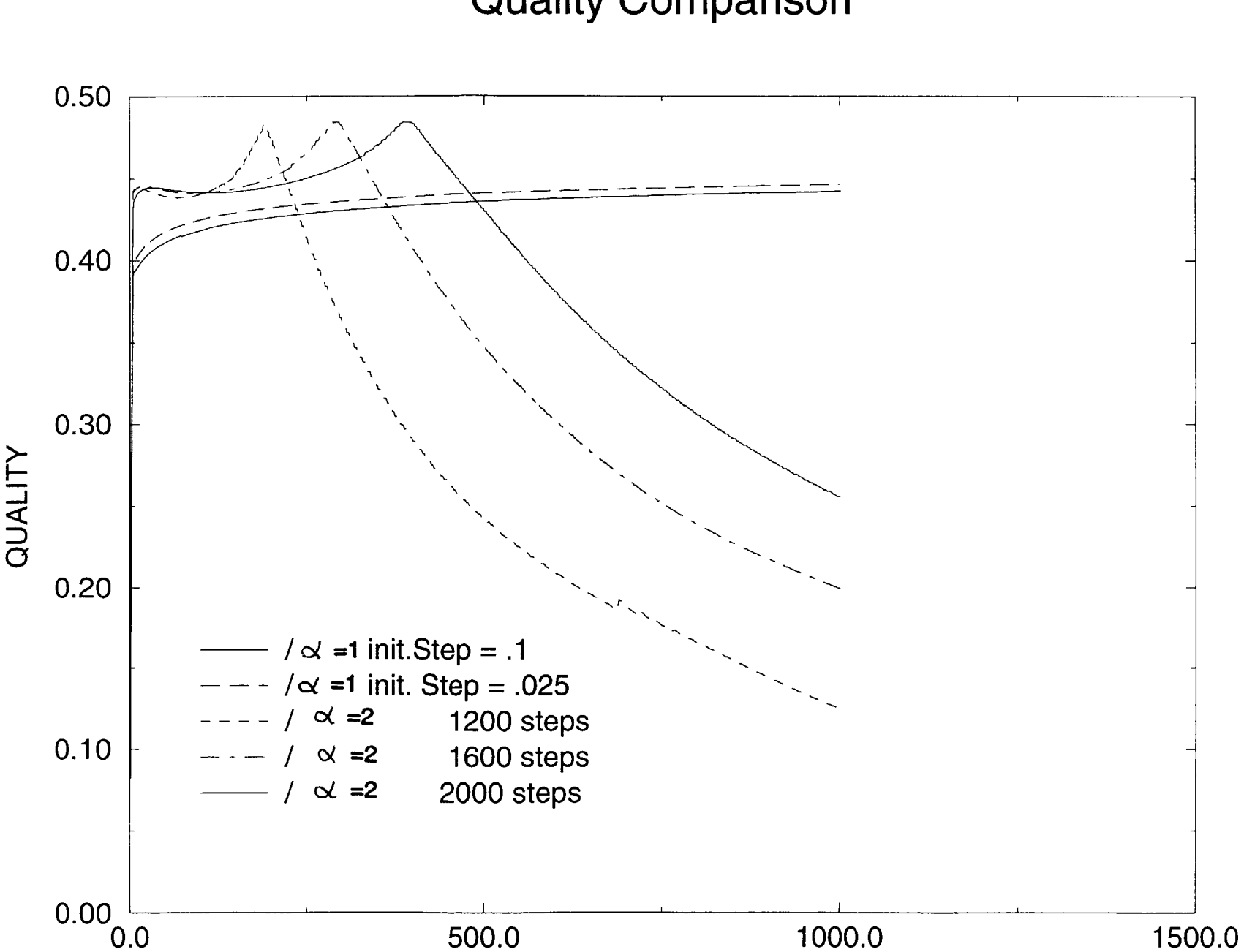

Figure 2. Mesh quality comparison for proposed formulation and other tested weighting factor.